SIMULATION OF COMPOSITE NON-LINEAR MECHANICAL BEHAVIOR OF CMCS BY FEM-BASED MULTI-SCALE APPROACH

Gao Xiguang(高希光), *Wang Shaohua*(王绍华), *Song Yingdong*(宋迎东)

(College of Energy and Power Engineering, Nanjing University of Aeronautics and Astronautics, Nanjing, 210016, P. R. China)

Abstract: The non-linear behavior of continuous fiber reinforced C/SiC ceramic matrix composites (CMCs) under tensile loading is modeled by three-dimensional representative volume element (RVE) models of the composite. The theoretical background of the multi-scale approach solved by the finite element method (FEM) is recalled firstly. Then the geometric characters of three kinds of damage mechanisms, i. e. micro matrix cracks, fiber/matrix interface debonding and fiber fracture, are studied. Three kinds of RVE are proposed to model the microstructure of C/SiC with above damage mechanisms respectively. The matrix cracking is modeled by critical matrix strain energy (CMSE) principle while a maximum shear stress criterion is used for modeling fiber/matrix interface debonding. The behavior of fiber fracture is modeled by the famous Weibull statistic theory. A numerical example of continuous fiber reinforced C/SiC composite under tensile loading is performed. The results show that the stress/strain curve predicted by the developed model agrees with experimental data.

Key words: ceramic-matrix composites (CMCs); mechanical properties; microstructure; computational modeling; micro-mechanics

CLC number: TB33 **Document code**: A **Article ID**: 1005-1120(2013)04-0328-07

INTRODUCTION

In the past years ceramic materials have become increasingly important because these materials combine the advanced behavior of ceramics such as high strength, high strength at elevated temperature and wearability with a non-brittle stress-strain behavior. However, ceramic composites are energetically prone to the formation of multiple matrix cracks prior to complete laminate failure. This, combined with the inherent complexities and stochastic nature of failure in non-homogeneous materials, makes the modeling of ceramic matrix composites (CMCs) quite difficult. Models have been presented by several authors to predict the critical stress at which the matrix cracks initiates[1-3]. In order to explain the stochastic feature of matrix cracking, Crutin et al. performed the study based on the statistic method[4-7]. Trying to simulate the whole response of ceramic composites, Solti[8] performed the study based on the shear lag method. However the shear lag method is too simple to calculate the microscopic stress field exactly. In addition to the model proposed by Solti, other models based on the continuum damage mechanics were proposed[9-10], which were however experiential.

In this paper, a comprehensive model relating the macro and micro response of unidirectional fiber toughened CMCs is proposed under tensile loading. The model describes the longitudinal strain response of C/SiC composite throughout the entire tensile test, taking into account all relevant damage. The mechanisms governing the

Website of on-first: **http**: // www. cnki. net/detail/32. 1389. V. 20121226、1652. 011. html(2012-12-26 16 : 52)

Foundation items: Supported by the National Natural Science Foundation of China (51075204, 51105195); the Aeronautical Science Foundation of China (2011ZB52024).

Received date: 2011-10-28; **revision received date**: 2012-02-17

Corresponding author: Gao Xiguang, Associate Professor, E-mail: gaoxiguang@nuaa. edu. cn.

non-linear response of the composite are the matrix cracking, fiber/matrix interface debonding and fiber fracture. The model is based on the multi-scale process[11-13] and is solved by the finite element method(FEM).

1 FEM-BASED MULTI-SCALE APPROACH

Considering a composite wherein the microstructure is periodically distributed in the axis directions (Fig. 1), where the representative volume element (RVE) used to construct the periodic array is highlighted. In the framework of Suquet [11], the displacements are decomposed as follows

$$u_i = \bar{\varepsilon}_{ij} X_j + \tilde{u}_i \qquad i,j = 1,2,3 \tag{1}$$

where $X=(X_1, X_2, X_3)$ is the macroscopic (global) coordinate, $u=(u_1, u_2, u_3)$ the displacement, $\bar{\varepsilon}_{ij}$ the global strain, $\tilde{u}_i$ the fluctuating displacement.

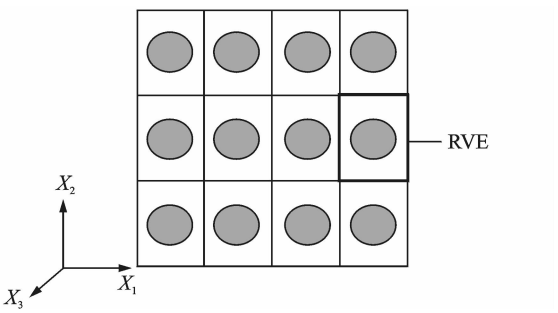

Fig. 1 Composite material with periodic microstructure

The global strain and stress are defined as the average of the local strain and stress within RVE, shown as

$$\bar{\varepsilon}_{ij} = \frac{1}{V}\int_{\Omega} \varepsilon_{ij}\,\mathrm{d}v, \bar{\sigma}_{ij} = \frac{1}{V}\int_{\Omega} \sigma_{ij}\,\mathrm{d}v \tag{2}$$

If the effect of body force is ignored, the virtual work principle has the following form

$$\int_{\Omega} \sigma_{ij}\delta\varepsilon_{ij}\,\mathrm{d}v = \int_{S_\sigma} T_i \delta u_i\,\mathrm{d}s \tag{3}$$

where Ω stands for the domain of RVE, and S_σ the stress boundary.

For the linear material, the constitutive equation is

$$\sigma_{ij} = E_{ijkl}\varepsilon_{kl} \tag{4}$$

Substitution of Eq. (4) into Eq. (3) gives that

$$\int_{\Omega} E_{ijkl}\varepsilon_{kl}\delta\varepsilon_{ij}\,\mathrm{d}v = \int_{S_\sigma} T_i \delta u_i\,\mathrm{d}s \tag{5}$$

The Cauchy infinitesimal strain tensor is defined as

$$\varepsilon_{ij} = \frac{1}{2}(u_{i,j} + u_{j,i}) \tag{6}$$

Substitution of Eq. (1) into Eq. (6) gives that

$$\varepsilon_{ij} = \bar{\varepsilon}_{ij} + \tilde{\varepsilon}_{ij} \tag{7}$$

where

$$\tilde{\varepsilon}_{ij} = \frac{1}{2}(\tilde{u}_{i,j} + \tilde{u}_{j,i}) \tag{8}$$

Substitution of Eqs. (1,7) into Eq. (5) gives that

$$\int_{\Omega} (E_{ijkl}\bar{\varepsilon}_{kl}\delta\bar{\varepsilon}_{ij} + E_{ijkl}\bar{\varepsilon}_{kl}\delta\tilde{\varepsilon}_{ij} + E_{ijkl}\tilde{\varepsilon}_{kl}\delta\bar{\varepsilon}_{ij} + E_{ijkl}\tilde{\varepsilon}_{kl}\delta\tilde{\varepsilon}_{ij})\,\mathrm{d}v = \int_{S_\sigma} (T_i\delta\bar{\varepsilon}_{ij}X_j + T_i\delta\tilde{u}_i)\,\mathrm{d}s \tag{9}$$

The global strain keeps constant in the process of deformation. Therefore the variation of $\bar{\varepsilon}_{ij}$ is zero. Eq. (9) becomes

$$\int_{\Omega} (E_{ijkl}\bar{\varepsilon}_{kl}\delta\tilde{\varepsilon}_{ij} + E_{ijkl}\tilde{\varepsilon}_{kl}\delta\tilde{\varepsilon}_{ij})\,\mathrm{d}v = \int_{S_\sigma} T_i\delta\tilde{u}_i\,\mathrm{d}s \tag{10}$$

The domain is discretized into a set of elements and the shape function ${}^eN^p$ is defined on each element. Then Eq. (10) becomes

$$\sum_e \int_{e_\Omega} (E_{ijkl}\bar{\varepsilon}_{kl}\delta\tilde{\varepsilon}_{ij} + E_{ijkl}\tilde{\varepsilon}_{kl}\delta\tilde{\varepsilon}_{ij})\,\mathrm{d}v = \sum_e \int_{e_S} T_i\delta\tilde{u}_i\,\mathrm{d}s \tag{11}$$

Then the fluctuating displacement and variation of fluctuating displacement are approximated by linear combinations of their nodal values and shape functions, namely

$${}^e\tilde{u}_i = {}^eN^p\,{}^e\tilde{u}_i^p,\ \delta{}^e\tilde{u}_i = {}^eN^p\delta{}^e\tilde{u}_i^p \tag{12}$$

Then the fluctuating strain becomes

$${}^e\tilde{\varepsilon}_{ij} = \frac{1}{2}{}^eN^p_{,j}\,{}^e\tilde{u}_i^p + \frac{1}{2}{}^eN^p_{,i}\,{}^e\tilde{u}_j^p \tag{13}$$

where

$${}^eN^p_{,j} = \frac{\partial {}^eN^p}{\partial x_j} \tag{14}$$

Combination of Eqs. (11—13) gives that

$$\sum_e \int_{e_\Omega} \left(E_{ijkl}\bar{\varepsilon}_{kl}\,\frac{1}{2}{}^eN^p_{,j}\delta{}^e\tilde{u}_i^p + E_{ijkl}\bar{\varepsilon}_{kl}\,\frac{1}{2}{}^eN^p_{,i}\delta{}^e\tilde{u}_j^p\right)\mathrm{d}v + \sum_e \int_{e_\Omega} E_{ijkl}\left(\frac{1}{2}{}^eN^q_{,l}\,{}^e\tilde{u}_k^q + \frac{1}{2}{}^eN^q_{,k}\,{}^e\tilde{u}_l^q\right)\times \left(\frac{1}{2}{}^eN^p_{,j}\delta{}^e\tilde{u}_i^p + \frac{1}{2}{}^eN^p_{,i}\delta{}^e\tilde{u}_j^p\right)\mathrm{d}v =$$

$$\sum_e \int_{e_S} T_i^e N^p \delta^e \tilde{u}_i^p \mathrm{d}s \tag{15}$$

Simplification of Eq. (15) gives that

$$\sum_e {}^e\tilde{u}_k^q {}^eK_{kqip} \delta^e \tilde{u}_i^p + \sum_e {}^e\bar{\varepsilon}_{kl} {}^eC_{klip} \delta^e \tilde{u}_i^p = \sum_e {}^eT_{ip} \delta^e \tilde{u}_i^p \tag{16}$$

where

$${}^eK_{kqip} = \int_{e_\Omega} K_{kqip} \mathrm{d}v \tag{17a}$$

$${}^eC_{klip} = \frac{1}{2} \int_{e_\Omega} (E^e_{ijkl} N^p_{,j} + E^e_{jikl} N^p_{,j}) \mathrm{d}v \tag{17b}$$

$${}^eT_{ip} = \int_{e_S} T_i^e N^p \mathrm{d}s \tag{17c}$$

$$K_{kqip} = \frac{1}{4} E^e_{ijkl} N^q_{,l} {}^e N^p_{,j} + \frac{1}{4} E^e_{ijlk} N^q_{,l} {}^e N^p_{,j} + \frac{1}{4} E^e_{jikl} N^q_{,l} {}^e N^p_{,j} + \frac{1}{4} E^e_{jilk} N^q_{,l} {}^e N^p_{,j} \tag{17d}$$

If the periodic boundary conditions are employed, the relation between global strains and nodal values of fluctuating displacement are given by the solution of Eq. (16), which has the following form

$${}^e\tilde{u}_k^p = {}^eKC_{kpmn} \bar{\varepsilon}_{mn} + {}^eU_k^p \tag{18}$$

where ${}^eKC_{kpmn}$ is the component of a four-order tensor and decided by the material properties and the shape of element, ${}^eU_k^p$ the component of a two-order tenser and decided by the stress boundary conditions.

The integral is performed in each element. Then global stress becomes

$$\bar{\sigma}_{ij} = \frac{1}{V} \sum_e \frac{{}^eV {}^eE_{ijkl}}{{}^eV} \int_{e_\Omega} \varepsilon_{kl} \mathrm{d}v = \sum_e \frac{{}^eV {}^eE_{ijkl} (A_{kl} + {}^e\bar{\varepsilon}_{kl})}{V} \tag{19}$$

where ${}^e\bar{\varepsilon}_{kl}$ is the average strain of element and defined as

$${}^e\bar{\varepsilon}_{kl} = \frac{1}{{}^eV} \int_{e_\Omega} \tilde{\varepsilon}_{kl} \mathrm{d}v \tag{20}$$

Substitution of Eq. (12) into Eq. (20) gives that

$${}^e\bar{\varepsilon}_{kl} = \frac{1}{{}^eV} \int_{e_\Omega} \left(\frac{1}{2} {}^e N^p_{,l} {}^e\tilde{u}_k^p + \frac{1}{2} {}^e N^p_{,k} {}^e\tilde{u}_l^p \right) \mathrm{d}v = \frac{1}{2} {}^e\bar{N}^p_{,l} {}^e\tilde{u}_k^p + \frac{1}{2} {}^e\bar{N}^p_{,k} {}^e\tilde{u}_l^p \tag{21}$$

Then the global stress becomes

$$\bar{\sigma}_{ij} = \sum_e \frac{{}^eV}{V} ({}^eE_{ijkl} \bar{\varepsilon}_{kl} + {}^eE^e_{ijkl} \bar{N}^p_{,l} {}^e\tilde{u}_k^p) \tag{22}$$

Substitution of Eq. (18) into Eq. (22) gives that

$$\bar{\sigma}_{ij} = \sum_e \frac{{}^eV}{V} ({}^eE_{ijkl} \bar{\varepsilon}_{kl} + {}^eE^e_{ijmn} \bar{N}^p_{,n} {}^eKC_{mpkl} \bar{\varepsilon}_{kl} + {}^eE^e_{ijkl} \bar{N}^p_{,l} {}^eU_k^p) \tag{23}$$

Simplification of Eq. (23) gives that

$$\bar{\sigma}_{ij} = \bar{E}_{ijkl} \bar{\varepsilon}_{kl} + \bar{T}_{ij} \tag{24}$$

where

$$\bar{E}_{ijkl} = \sum_e \frac{{}^eV}{V} ({}^eE_{ijkl} + {}^eE^e_{ijmn} \bar{N}^p_{,n} {}^eKC_{mpkl}) \tag{25}$$

$$\bar{T}_{ij} = \sum_e \frac{{}^eV}{V} ({}^eE^e_{ijkl} \bar{N}^p_{,l} {}^eU_k^p) \tag{26}$$

Eq. (25) gives the formulation of effective elastic tenser of material.

2 DAMAGE MECHANISMS AND MODELING

In CMCs continuous cylindrical fibers are embedded in a high performance ceramic matrix which is typically some derivatives (oxide, nitride, or carbide) of silicon, aluminum, titanium or zirconium. An example is C/SiC CMCs which embed small diameter carbide fibers into a carborundum matrix. CMCs exhibit a remarkable increase in toughness compared with their monolithic counterparts.

The degree of toughening exhibited by CMCs is a function of the strength of the interface, the frictional of shear resistance within debonded regions and the strength of the matrix and fiber. In order to describe the train response of CMCs under a tensile test, three damage mechanisms which are micro-cracking of matrix, fiber/matrix interface debonding and fiber fracture are employed in this model. The model consists of a rectangular array of perfectly aligned fibers in a matrix (Fig. 1). The thickness of the interphase between fiber and matrix is assumed to be negligible.

2.1 Matrix failure

Previous work on unidirectional fiber toughened CMCs has indicated that during tensile stressing matrix cracks develop into more or less periodic arrays, with a characteristic spacing. The proposed model assumes the cracks to be equidistant and spanning the entire cross section

of the material. The crack distance L is determined by the critical matrix strain energy (CMSE) approach [14-15]. In general, the CMSE criterion states that matrix cracking at any strain level ε with the average crack spacing of L and a fiber/matrix length d (Fig. 2) will occur when the matrix strain energy is equal to its critical value, U_{crm}, i. e.

$$U_m = U_{crm} \tag{27}$$

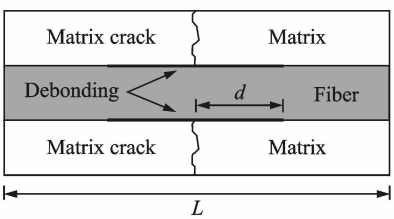

Fig. 2 Definition of L and d in RVE

CMSE, U_{crm}, is defined as the strain energy in the matrix at the critical composite stress, σ_{cr}. That means U_m keeps constant and equals to U_{crm} at any stress lever which is greater than σ_{cr}. However, the initial crack spacing, L_{init}, at $\sigma = \sigma_{cr}$, must be determined for the CMSE failure criterion. For the current analysis, the initial crack spacing is chosen such that the strain energy of the damaged configuration is "close" to the strain energy in the undamaged configuration U_{m0}. For example, the deviation is three percent (i. e. $U_{crm} = 0.97U_{m0}$). U_{m0} is the matrix strain energy calculated by

$$U_{m0} = L_{init} \cdot S_m \cdot E_m \cdot \left(\frac{\sigma_{cr}}{E_c}\right)^2 \tag{28}$$

where S_m is the area of matrix, E_m the elastic modulo of matrix, E_c the elastic modulo of composite, which is

$$E_c = v_f E_f + v_m E_m \tag{29}$$

where v_f , v_m are the volume fraction of the fiber and matrix. For the present study, a constant deviation of one percent is used for all cases, that is

$$U_{crm} = 0.99U_{m0} \tag{30}$$

2.2 Interface debonding

As matrix cracks form within the composite, they can also induce interface debonding. These usually result from the large stress fields near the matrix crack-tip. Since the debonding is in reality a crack which propagates along the fiber/matrix interface, the extent of debonding can be estimated using classical fracture mechanics techniques[16-18]. However, to avoid the complexities which accompany such approaches, a simple and more common approach is to employ a maximum stress criterion in which the debonding occurs whenever the interface shear stress exceeds the ultimate bond strength of the interface, τ_{ult} [1,19,20]. The parameter τ_{ult} is assumed to be a material constant, and, if known, the extent of interface debonding can be determined by ensuring that the maximum shear along the interface never exceeds this maximum amount, i. e.

$$\tau_i(x)_{max} = \tau_{ult} \tag{31}$$

The shear stress in the debonding region is typically assumed to be constant and governed by Coulomb friction with magnitude τ_i [20-21].

2.3 Fiber fracture

The percentage of fracture fibers, f, in CMCs is typically determined using some type of statistical failure criterion. The most common approach is to use a two-parameter Weibull distribution like the following.

$$f = 1 - \exp\left\{\left(\frac{\sigma}{\sigma_0}\right)^m\right\}^{-1} \tag{32}$$

where σ_0 is the characteristic fiber strength and m the tradition Weibull modulus. From Eq. (32), σ_0 corresponds to a survival probability of 0.37%. The shape and scaling parameters, m and σ_0, may be determined by fitting empirical data; however, their solution is somewhat involved since the variation in f versus σ cannot be solved directly.

2.4 Simulation of damage process

The modeling process is divided into four steps:

(1) Before damage developing, the composite is represented by a perfect RVE (Fig. 3 (a)). At this step, the material is elastic, and the global behavior is described by Eq. (29).

(2) When the matrix cracking occurs and the interface is perfect, the configuration of RVE is presented by Fig. 3 (b). At this step, the crack space is determined by

$$U_m(L) = U_{crm} \tag{33}$$

(3) In the presence of matrix cracking and partially debonded interfaces, the composite is described by a corresponding RVE with a matrix crack and a partially debonding interface (Fig. 3 (c)). The crack space and debonding length are determined by

$$U_m(L,d) = U_{crm},\ \tau_{max}(L,d) = \tau_{ult} \tag{34}$$

where d denotes the debonding length of interface, and τ_{ult} the shear strength of the perfect interface.

(4) When d is close to $L/2$, the configuration of RVE is presented by Fig. 3 (d). In this case, the behavior of the composite is dominated by

$$\sigma_f - f \cdot v_f \cdot E_f \cdot \bar{\varepsilon} = 0 \tag{35}$$

where σ_f denotes the fiber stress while v_f the volume fraction of fiber.

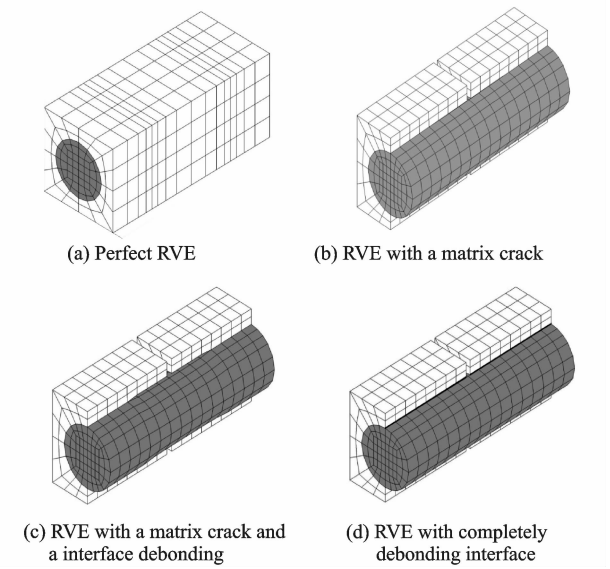

Fig. 3 Configurations of RVE at each damage state

3 FINITE ELEMENT RESULTS AND DISCUSSION

The constituent properties used for the simulation are summarized in Table 1. RVE is loaded by uniaxial tensile stress in fiber direction. The initial linear elastic behavior ends because of the crack initiation in the matrix and the debonding of interface.

Table 1 Material property data of C/SiC

Material property	Value	Material property	Value
E_f/GPa	230	E_m/GPa	116.2
μ_f	0.21	μ_m	0.24
v_f	0.40	R_f/μm	7.5
τ_{ult}/MPa	50	σ_{cr}/MPa	126.4
m	4.0	σ_0/MPa	323

When the debonding length is close to $L/2$, the fiber fracture occurs. Then there is a reduction of the elastic coefficients of the fiber. The experimentally determined points[22] and simulated results are given in Fig. 4, where the range between A and B is linear because RVE is perfect. For higher loading of RVE, matrix cracking initiates and the interface debonding occurs (B-C). In the range between C and D, the matrix cracks saturate because the matrix cannot receive enough energy from fiber since the interface debonding. In this range interface debonding is the only damage mechanism which dominates the behavior of the material. As load increases, the interface debonding length approaches $L/2$ and the fiber fracture dominates the mechanics behavior of the composite (D-E). The curves of matrix crack space and interface debonding length which are calculated by the model are shown in Fig. 5.

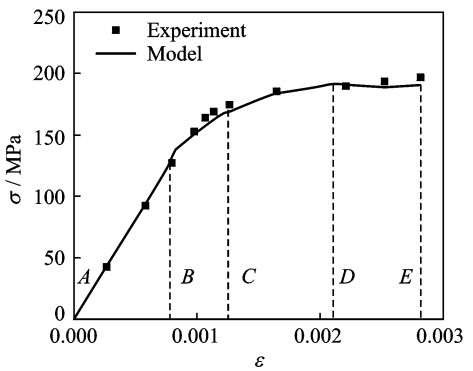

Fig. 4 Stress-strain predictions from current analysis along with experimental values

4 CONCLUSION

A FEM-based multi-scale approach is proposed to simulate the non-linear mechanical behavior of ceramic matrix composite. The present results suggest that:

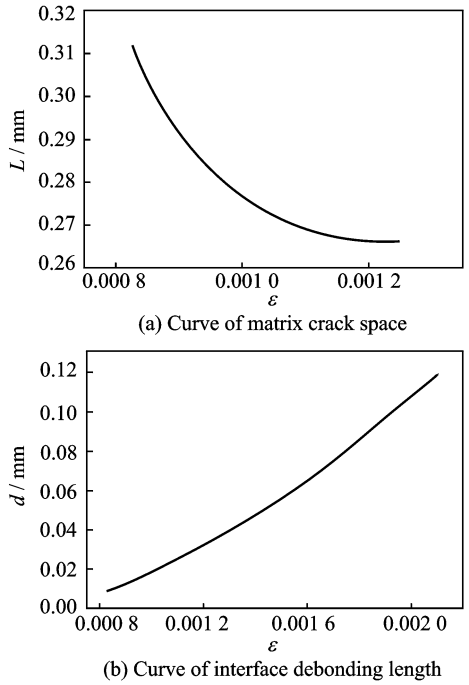

Fig. 5 Curves of microscopic damage parameters

(1) The stress-strain response predicted by the model proposed in this paper is fit quite well with the experience.

(2) Fiber reinforced CMC is an approximate linear composite if there is no damage. The stiffness of CMC declines when the damage appears.

(3) The matrix cracking, interface debonding and fiber fracture are the basic damage mechanism of ceramic composites. When the external load exceeds the critical stress, matrix cracking initiates and then the interface debonding occurs.

(4) The matrix cracks saturate because the matrix cannot receive enough energy from fiber because of the interface debonding. In this range interface debonding is the only damage mechanism which dominates the material behavior .

(5) As load increases, the interface debonding length approaches half of the distance between adjacent matrix cracks, and the fiber fracture will be the main factor affecting the mechanics behavior of the composite.

References:

[1] Aveston J, Cooper G A, Kelly A. Single and multiple fracture, the properties of fiber composites[C]// Conference Proceedings on the Properties of Fiber Composites. Guildford, UK: IPC Science and Technology Press Ltd, 1971: 15-26.

[2] Budiansky B, Hutchinson J W, Evans A G. Matrix fracture in fiber-reinforced ceramics[J]. Journal of Mechanics Physical Solids, 1986, 34(2):167-189.

[3] Marshall D B, Evans A G. Failure mechanisms in ceramic-fiber/ceramic-matrix composites[J]. Journal of American Ceramic Society, 1985, 68 (5): 225-231.

[4] Curtin W A. Exact theory of fiber fragmentation in a single-filament composite[J]. Journal of Materials Science, 1991, 26(19): 5239-5253.

[5] Curtin W A. Theory of mechanical properties of ceramic-matrix composites[J]. Journal of American Ceramic Society, 1991, 74(11): 2837-2845.

[6] Ahn B K, Curtin W A. Strain and hysteresis by stochastic matrix cracking in ceramic matrix composites [J]. Journal of Mechanics Physical Solids, 1997, 45: 177-209.

[7] Curtin W A, Ahn B K, Takend N. Modeling brittle and tough stress-strain behavior in unidirectional ceramic matrix composites[J]. Acta Material, 1998, 46(10): 3409-3420.

[8] Solti J P. Modeling of progressive damage in fiber reinforced ceramic matrix composites[D]. USA: Air Force Inst of Tech Wright-Patterson AFB (Ohio) School of Engineering, 2005.

[9] Chaboche J L, Maire J F. A new micromechanics based CDM model and its application to CMCs[J]. Aerospace Science and Technology, 2002, 6(2): 131-145.

[10] Chaboche J L, Maire J F. New progress in micromechanics-based CDM models and their application to CMCs [J]. Composites Science and Technology, 2001,61(15): 2239-2246.

[11] Moulinec H, Suquet P. Effective properties of composite materials with periodic microstructure: A computational approach[J]. Computer Methods in Applied Mechanics and Engineering, 1998,157 (1/2): 69-94.

[12] Sanchez-Palencia E. Non-homogeneous media and vibration theory[M]. Berlin:Springer-Verlag, 1980.

[13] Bensoussan A, Lions J L, Papanicolaou G. Asymptotic analysis for periodic structures[M]. Amesterdam: North-Holland Pub Co, 1978.

[14] Solti J P, Mall S, Robertson D D. Modeling damage in unidirectional ceramic matrix composites[J]. Composites Science and Technology, 1995, 54(1):55-66.

[15] Solti J P, Mall S, Robertson D D. Modeling of progressive damage in unidirectional ceramic matrix

composites[J]. Composites Science and Technology, 1995,54(1):55-66.

[16] Charalambides P G. Fiber debonding in residually stressed brittle matrix composites[J]. Journal of the American Ceramic Society, 1990, 73 (6): 1674-1680.

[17] Dharani L R, Fangsheng J. 3-D shear lag model for the analysis of interface damage in ceramic matrix composites[C]// Recent Advances in Composite Materials, Joint Applied Mechanics and Materials Summer Conference. Los Angeles, California: ASME, 1995:47-56.

[18] Hutchison J W, Jensen H M. Models of fiber debonding and pullout in brittle composites with friction[J]. Mechanics of Material, 1990, 9(2): 139-163.

[19] Cho C, Holmes J W, Barber J R. Estimation of interfacial shear in ceramic composites from frictional heating measurements[J]. Journal of American Ceramic Society, 1991, 74 (11):2802-2808.

[20] Lee J W, Daniel I M. Deformation and failure of longitudinally loaded Brittle-matrix composites [C]// Proceedings of the Tenth Symposium on Composite Materials: Testing and Design. Grimes G C Ed. [S. l.]:ASTM, 1992:204-221.

[21] Kuo W S. Damage of multi-directionally reinforced ceramic matrix composites[D]. USA: Department of Mechanical Engineering, University of Delaware, 1992.

[22] Solti J P. Modeling of progressive damage in fiber-reinforced ceramic matrix composites[M]. USA:Storming Media, 1996.